

## Chapter 2

# Theoretical Study of Continuous-Time Equalizers

In this chapter, the principles of continuous-time adaptive equalization will be explored. First, basic theory of continuous-time equalization will be analyzed, focusing on its transfer function and how it should compensate the response of the channel. Second, the power spectrum characteristics of the transferred data will be analyzed, focusing on the non-return-to-zero (NRZ) data encoding and pseudo random bit sequence (PRBS), which is the typical signal used to test serial communication prototypes. Next, a thorough and unified analysis of continuous-time adaptive equalizers that will lead to a set of design criteria to select the proper bandwidth of the filters used in the adaptation loop will be presented. It has into account the characteristics of the communications system such as the data rate, channel bandwidth and the specific line equalizer used. After this analysis, a functional simulation of continuous-time adaptive equalizers will be presented to determine which filters are preferred in the adaptation loop. Finally, some conclusions of the chapter will be drawn.

### 2.1 Basic Theory

The effect of the channel on the signal can be divided into two categories. On the one hand, the signal is corrupted with noise, which results in decreased signal-to-noise ratio (SNR) and in timing jitter; these two effects are compensated at the clock and data recovery circuit (CDR) [SAN11]. On the other hand, the limited channel bandwidth causes the transitions of the data stream to lose sharpness due to the attenuation experienced by high frequency components. This also increases the intersymbol interference (ISI), thereby reducing the opening of the eye diagram and increasing the bit error rate (BER): these softer transitions take longer to complete, which causes the value of each bit of information to be affected by its neighbors [HOL06]. As explained in the previous chapter, equalization is a technique which is widely used to reduce ISI.

The relationship between the Laplace transforms of the received data  $R(s)$  and the transmitted data  $T(s)$  can be described by the following equation

$$R(s) = H_{Ch}(s) \cdot T(s) \quad (2.1)$$

ISI is contained in  $H_{Ch}(s)$ , which describes how a signal is affected by the channel. The ideal equalizer comes from the inverse of the transfer function, so it receives the signal back just as it was transmitted (except for random noise):

$$H_{Ch}^{-1}(s) \cdot H_{Ch}(s) \cdot T(s) = H_{Ch}^{-1}(s) \cdot R(s) = T(s) \quad (2.2)$$

Consider that the channel can be modeled as a linear time-invariant system with a frequency response with a dominant pole  $p_{Ch}$ . Its approximate frequency response is

$$H_{Ch}(s) = A_{Ch}(s) \cdot \frac{1}{\left(1 + \frac{s}{p_{Ch}}\right)} \quad (2.3)$$

Where all the rest of the frequency dependency is included in  $A_{Ch}(s)$ .

To overcome the extreme frequency limitations caused by the channel, the equalizer has to boost the frequency components of the incoming signal which are just above its BW; in this way, an equalizer produces an effective extension of the receiver bandwidth beyond the one inherent to the channel. So the transfer function of the equalizer must not only have at least one zero placed close to the channel pole to neutralize its effect, but also at least one pole in order to be feasible.

The transfer function of the equalizer  $H_{Eq}(s)$  is given by

$$H_{Eq}(s) = A_{Eq}(s) \cdot \frac{1 + \frac{s}{z_{Eq}}}{\left(1 + \frac{s}{p_{Eq}}\right)} \quad (2.4)$$

where  $z_{Eq}$  and  $p_{Eq}$  are the zero and the dominant pole, respectively, of the line equalizer. So, the net effect of the channel and the equalizer can be written as

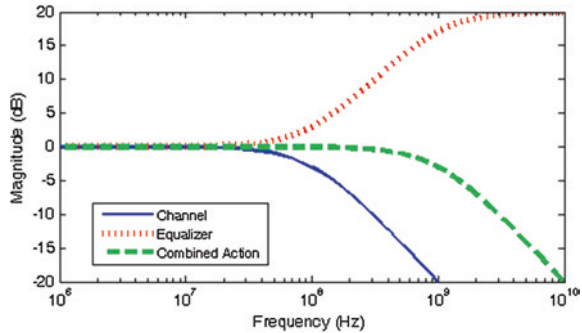
$$H_T(s) = A_{Ch}(s) \cdot \frac{1}{\left(1 + \frac{s}{p_{Ch}}\right)} \cdot A_{Eq}(s) \cdot \frac{\left(1 + \frac{s}{z_{Eq}}\right)}{\left(1 + \frac{s}{p_{Eq}}\right)} \quad (2.5)$$

Optimal equalization happens when the zero of the line equalizer cancels the channel pole ( $z_{Eq} = p_{Ch}$ ). This way

$$H_T(s) = A_{Ch}(s) \cdot A_{Eq}(s) \cdot \frac{1}{\left(1 + \frac{s}{p_{Eq}}\right)} \quad (2.6)$$

The line equalizer main pole gives the BW of the whole channel-equalizer combination in the dominant pole approach. For this reason, it must be higher than the

**Fig. 2.1** Typical smoothed frequency response of the channel (*line*), the equalizer (*pointed*) and the frequency response of their combined action (*dashed*)



channel pole and large enough for the system to operate correctly at the intended bit rate. Figure 2.1 shows the effect of equalization.

## 2.2 Power Spectral Density of NRZ Data Encoding

NRZ signaling is widely used for data transmission in digital communication systems. In NRZ signaling, each binary bit is assigned a unique time slot of duration, referred to as the bit period ( $T_B$ ), and therefore the bit rate ( $R_B$ ) of the signal (number of pulses transmitted in one second) is  $R_B = 1/T_B$ . The signal is either high (representing a one) or low (representing a zero) over the entire bit period.

For a random NRZ data stream, each bit in the sequence has an equal probability (50 %) of being a one or a zero, regardless of the state of the preceding bits. It is therefore possible to have large sequences of consecutive identical digits. Long sequences of identical digits produce a very low frequency content which requires a good low bandwidth limit making designing high-speed systems more complicated. Moreover, because of the slow signal transition density, the ac coupling, offset cancellation and clock recovery can create operation problems as they are sensitive to low densities transmission.

A PRBS is used as a general-purpose test pattern in NRZ applications. The PRBS is typically denoted as a  $2^N - 1$  PRBS, where  $N$  indicates the shift register length used to create the pattern. Each  $2^N - 1$  PRBS contains every possible combination of  $N$  number of bits (except one).

Each NRZ test pattern has an associated power spectral density (PSD). Two methods exist for computing the PSD: (a) squaring the magnitude of the Fourier transform of the pattern; or (b) computing the Fourier transform of the pattern autocorrelation function [GOO85]. The first method is generally simpler for signals that can be mathematically written in a finite, closed form, such as sinusoidal signals. The second method is used for more complicated signals, such as long sequences of NRZ data (like test patterns) or random bit stream.

It can be argued that the autocorrelation of an ideal NRZ random data stream with a bit period equal to  $T_B$  is non-zero only when the bits superimpose each other due to the random nature of the signal so that it resembles a triangular

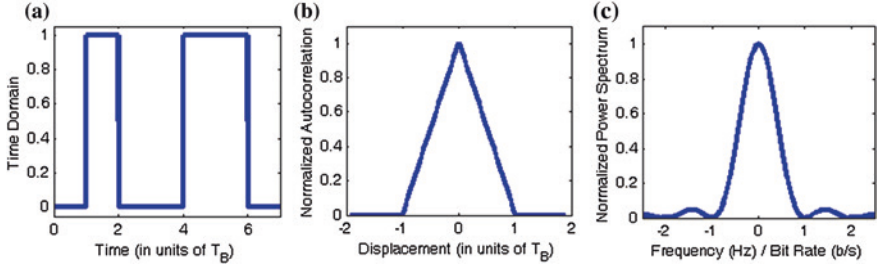


**Fig. 2.2** Ideal NRZ test pattern illustrated in **a** time domain, **b** autocorrelation of it, and **c** power spectrum of it

function extending from  $-T_B$  to  $T_B$  [HAY01]. Its Fourier transform is a  $\text{sinc}^2$  function. Figure 2.2 illustrates this.

So, the PSD,  $S(f)$ , of an ideal NRZ random data stream with period  $T_B$  is

$$S(f) = T_B \cdot \text{sinc}^2(\pi \cdot f \cdot T_B) = T_B \cdot \left( \frac{\sin(\pi \cdot f \cdot T_B)}{\pi \cdot f \cdot T_B} \right)^2 \quad (2.7)$$

A signal as random as possible must be generated for test purposes. However, software and hardware sequence generators are based on recurrence rules, so the generated signal is not strictly random. The PRBS spectrum is the combination of the ideal NRZ spectrum and a delta train with a period equal to  $N \cdot T_B$ . The delta train transform is also a delta train, but the period is equal to  $R_B/(2^N - 1)$ , and therefore, the  $\text{sinc}^2$  function is now restricted to certain frequencies. Figure 2.3 shows the PSD of a PRBS with different pattern lengths. Thus, the PRBS signal behaves like a random signal due to the lack of correlation within the pattern if its length is adequately high.

Finally, as mentioned, the channel behaves like a low-pass filter (LPF) filtering the signal and modifying the spectrum; moreover, if the equalizer is wrongly tuned, it can over-boost the signal, acting as a high-pass filter (HPF) for the PSD of the NRZ signal. Therefore, it can be illustrative to show how LPF or HPF affects the spectrum of an ideal NRZ signal. Figure 2.4 shows this effect.

### 2.3 Unified Model for CT Equalizers in the Frequency Domain

The frequency response of a typical communication channel is a complex function of its length, the frequency of the transmitted signal and other material properties of the channel [HOO04]. This function depends greatly on the specific channel; however, for a theoretical analysis, it is sufficient to describe the channel by a first-order LPF [BEY08, HOO04, YOO06]. We suppose that the normalized transfer function of the channel  $H_{Ch}(s)$  is given by

$$H_{Ch}(s) = \frac{1}{1 + \frac{s}{p_{Ch}}} \quad (2.8)$$

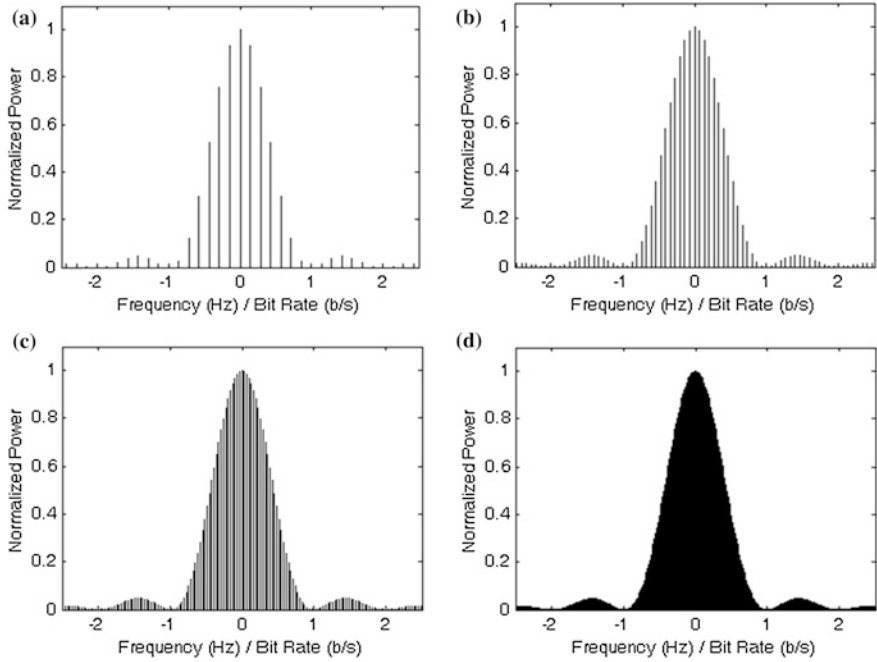
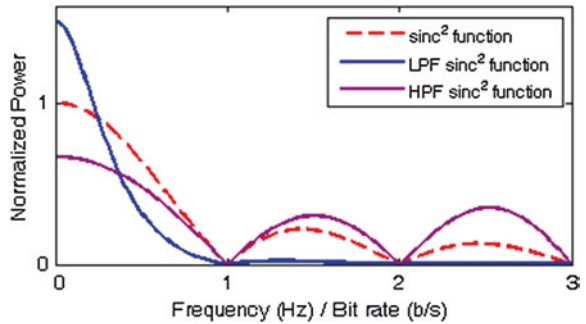


**Fig. 2.3** PSD of a  $2^N - 1$  PRBS with **a**  $N = 3$ , **b**  $N = 4$ , **c**  $N = 5$ , and **d**  $N = 6$

**Fig. 2.4** Normalized power spectral density of a NRZ data stream and how different filtering modifies it. The three spectrums have the same total power



In the specific application of the work, the BW of the SI-POF channel ranges from about 100 MHz for 50-m length to roughly 400 MHz for 10-m length. Figure 2.5 shows the power spectrum of the NRZ data stream after passing through the channel along with the power spectrum of an ideal NRZ data stream. Furthermore, in this book we are working with split-path continuous-time equalizers. The model for a split-path equalizer is given in Fig. 2.6, where the all-pass filter has been substituted by a shortcut to simplify the calculations. The high-pass filter has a pole at  $p_{Eq}$  and a boosting gain  $A$ . Its normalized transfer function  $H_{Eq}(s)$  is given by

**Fig. 2.5** PSD of an ideal NRZ data stream and PSD of the data stream out of the channel

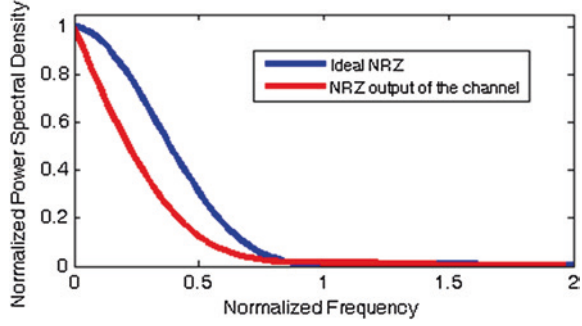
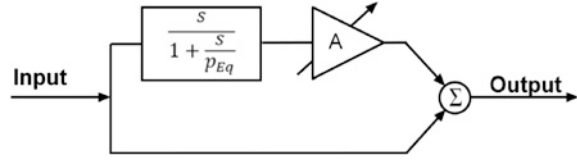


**Fig. 2.6** Line equalizer block diagram



$$H_{Eq}(s) = \frac{1 + s \cdot \frac{1 + A \cdot p_{Eq}}{p_{Eq}}}{1 + \frac{s}{p_{Eq}}} \quad (2.9)$$

And the combined frequency response of the channel and equalizer can be written as

$$H_T(s) = H_{Ch}(s) \cdot H_{Eq}(s) = \frac{1}{1 + \frac{s}{p_{Ch}}} \cdot \frac{1 + s \cdot \frac{1 + A \cdot p_{Eq}}{p_{Eq}}}{1 + \frac{s}{p_{Eq}}} \quad (2.10)$$

To obtain optimal equalization the zero of the line equalizer should compensate the channel pole. Looking back at (2.8) and (2.9), the optimal boosting gain is equal to

$$A_{Opt} = \frac{p_{Eq} - p_{Ch}}{p_{Eq} \cdot p_{Ch}} \quad (2.11)$$

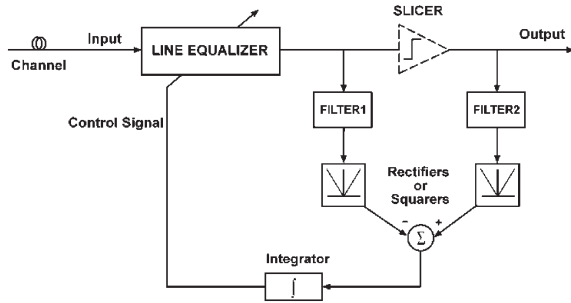
When optimal equalization has been achieved, (2.9) can be written as

$$H_{Eq}(s) = \frac{1 + \frac{s}{p_{Ch}}}{1 + \frac{s}{p_{Eq}}} = \frac{p_{Eq} \cdot s + p_{Eq} \cdot p_{Ch}}{p_{Ch} \cdot s + p_{Eq} \cdot p_{Ch}} \quad (2.12)$$

Finally, the combined frequency response of the channel and equalizer for optimal equalization can be written as

$$H_T(s)|_{A_{Opt}} = \frac{1}{1 + \frac{s}{p_{Eq}}} \quad (2.13)$$

**Fig. 2.7** Conceptual scheme of the adaptive equalizers with and without slicer



$H_T(s)|_{A_{Opt}}$  depends only on the position of the main equalizer pole, which is a natural consequence of the fact that optimal equalization has been achieved.

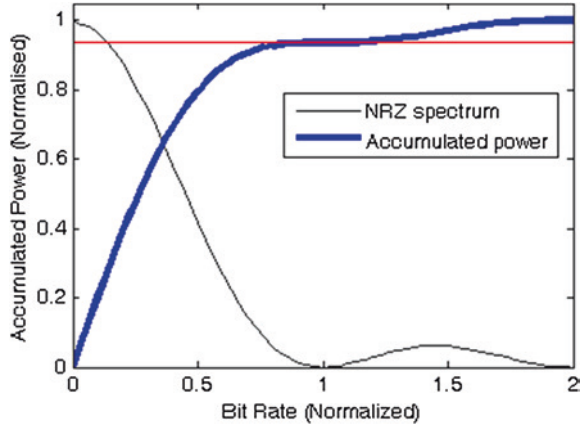
Moreover, the equalizer is required to be adaptive to compensate the variations of the channel characteristics, i.e., changes of the position of its pole. As explained in the previous chapter, two main architectures have been used for the design of the adaptation loop in continuous-time adaptive equalizers: architectures which use a slicer and architectures based on the spectrum-balancing technique. Figure 2.7 shows the adaptation loop block diagram including both alternatives. Both architectures compare the signal at the output of the equalizer with an ideal one (that comes from the output of the slicer or the ideal spectrum is known in advance). This is achieved by means of two filters and an error comparator which can be implemented in many different ways, such as by using rectifiers, or squarers. It is important to mention here, that the filters used to select the spectrum range are simple first order filters implemented with an RC circuit or as a simple Gm-C filter.

Typically, the design of the control loop of an adaptive equalizer using a slicer is carried out in the time domain; in contrast, adaptive equalizers based on the spectrum-balancing technique are analyzed in the frequency domain. We are going to show how, in both cases, a unified description in the frequency domain is valid.

Moreover, the specific BW of the filters used to separate the frequency regions for comparison is typically set ad hoc, after a trial and error process. We shall now present a thorough and unified analysis of continuous-time (CT) adaptive equalizers that will lead to a set of design criteria to select the proper filter bandwidth according to the characteristics of the communications system such as the data rate, channel BW, or the specific line equalizer used [SAN13, SAN14]. To provide a general analysis, all frequencies used will be normalized to the data bit rate.

As a first design criterion, it is important to mention that the bandwidth of any filter used to implement CT adaptive equalizers should be placed within the first lobe, no matter which architecture is used. To explain the reason behind this, we must first analyze the accumulated power of the PSD of an NRZ data stream (Fig. 2.8). It can be seen that the accumulation of power increases rapidly for frequencies close to zero. Then, as the frequency approaches  $1/T_B$ , the rate of power

**Fig. 2.8** NRZ PSD  
accumulated power



accumulation drops to zero, when it coincides with the first null of the PSD. Additionally, more than 90 % of the total power of the signal is concentrated within the first lobe. An extension of the bandwidth up to the next lobe ( $f = 2/T_B$ ) only increases the total power by less than 5 %.

To perform the calculations, typical numerical values for short-haul optical communication systems have been used. In particular, the data have been chosen to be a  $R_B = 1.25$  Gb/s NRZ data stream, the channel bandwidth has been set to 100 MHz (BW of a 50-m SI-POF), and the equalizer has been providing a 1.25 GHz bandwidth. These values yield an optimal gain for equalization of  $A_{Opt} \cong 9$ .

### 2.3.1 CT Adaptive Equalizer with a Slicer

In these kind of adaptive loops a slicer after the equalization filter further sharpens the transitions between the bits and therefore boosts the high-frequency content of the signal.

Although one might believe that the effect of the slicer, which is making bit transitions sharper, could suffice to overcome ISI and restore the data signal, this is not the case. To demonstrate this let us consider an ideal slicer and take into account only the filtering effect of the channel. At an ideal, when a transition takes place, its value changes from 1 to 0 or vice versa in a time which is theoretically zero. For a real signal affected by a low-pass filtering, this transition time increases as the filtering that the signal undergoes becomes more restrictive. Even if an ideal slicer were used to implement the equalizer, it should be ensured that the incoming signal has, in all cases, enough time to cross the comparison threshold before the following transition takes place.

In the case of a randomly varying signal such as NRZ modulated data stream, the worst case happens when a single bit is located in a long run of identical bits.

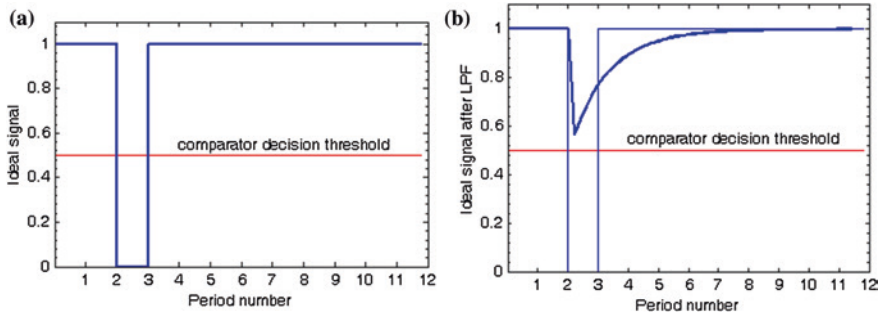


Fig. 2.9 a Ideal pulse and b ideal pulse after low-pass filtering

Figure 2.9 depicts this situation. It can be seen that, even if there is no noise or jitter affecting the signal, when sufficient restrictive low-pass filtering affects the signal, the single transition has not enough time to cross the threshold of the slicer. Therefore, it is necessary to include an adaptive equalizer even though a slicer is used in the loop structure. The operation principle of this type of CT adaptive equalizer is based on the fact that the transition time of the ideally equalized signal is known in advance; therefore, if a slicer is designed to produce an output with that given transition time, it can be used as a reference to determine whether the equalized signal is under- or over-compensated and adjust the equalizer accordingly [ZHA05].

The transition time<sup>1</sup> expected for the ideally equalized signal can be calculated by applying an ideal step to the combination of the channel and the equalizer transfer function particularized for  $A = A_{Opt}$ . If this is carried out with the previous model, the transition time  $t_{trans}$  is equal to

$$t_{trans} = \frac{1}{2 \cdot \pi \cdot p_{Eq}} \cdot \ln 4 \quad (2.14)$$

It can be seen that its value depends only on the dominant pole of the equalizer.

To understand why comparing time transitions is equivalent to a comparison of the spectral content of the signals both before and after the slicer, remember that the PSD of a signal is found by obtaining the Fourier transform of its autocorrelation [HAY01], which, in the case of an NRZ random data, is equal to a  $\text{sinc}^2$  function, as previously shown. This description becomes more accurate as the length of the bit stream tends towards infinity.

If we consider a real data signal with finite transition times, the shape of its autocorrelation deviates from that of the ideal signal. Figure 2.10a shows the triangular shape of the auto-correlation when the transition times range from 0 to  $T_B$ . We can see that it is smoothed and extends beyond  $\pm T_B$ . If its Fourier transform is obtained

<sup>1</sup> The transition time is defined as the time taken by the signal to change from a specified low value to a specified high value or vice versa. In our case, these values are 10 and 90 % of the step height.

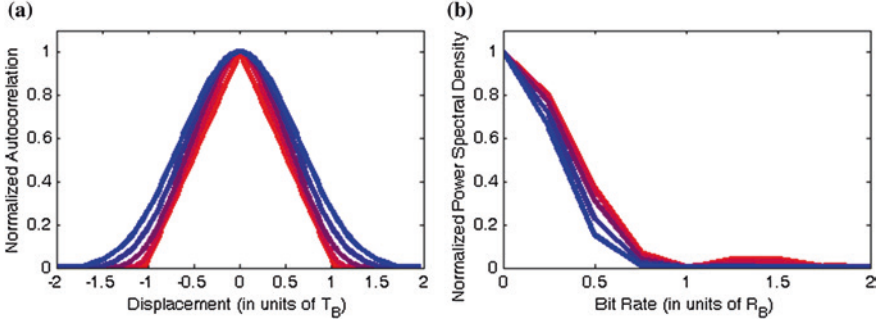


**Fig. 2.10** **a** Autocorrelation and **b** PSD of a random signal with transition times from 0 (red) to 100 % of the bit period (blue)

(Fig. 2.10b), the deviations from the triangular shape derived from the finite transition times result in variations in the PSD, especially for high frequency components, which appear over-attenuated.

In other words, it is possible to assimilate changes in the transition time of the signal (time domain description) to changes in PSD (frequency domain description); so, considering the PSD of the slicer output signal as the reference to drive the adaptation loop is equivalent to considering its transition time. This way, the adaptation loop can be closed by comparing a certain frequency range of the PSD at the input and output of the slicer; the choice of frequencies for PSD comparison must be made in order to maximize the sensitivity of the adaptation loop.

The PSD of the equalizer input signal is the combination of the PSD of the data stream (a  $\text{sinc}^2$  function) and the LPF that models the channel; the PSD of the equalizer output results from applying  $H_{Eq}(s)$  to its input.

The relationship between the power spectral densities at the input  $S_{in}(f)$  and the output  $S_{out}(f)$  of a system with a transfer function equal to  $H(f)$  is given by

$$S_{out}(f) = S_{in}(f) \cdot [H(jf)]^2 \quad (2.15)$$

As the input data stream passes first through the channel,  $H_{Ch}(s)$ , and then the equalizer,  $H_{Eq}(s, A)$ , we can relate the PSD of the equalizer output ( $S_{out,eq}(f, A)$ ) with that of the transmitted signal ( $S_{in}(f)$ ) by

$$\begin{aligned} S_{out,eq}(f, A) &= S_{in}(f) \cdot [H_{Ch}(jf)]^2 \cdot [H_{Eq}(jf, A)]^2 \\ &= \left( \frac{\sin(\pi \cdot f)}{\pi \cdot f} \right)^2 \cdot \frac{p_{Ch}^2}{f^2 + p_{Ch}^2} \cdot \frac{(1 + A \cdot p_{Eq})^2 \cdot f^2 + p_{Eq}^2}{f^2 + p_{Eq}^2} \end{aligned} \quad (2.16)$$

As the slicer is designed so that the transition times of its output are those expected for the ideally equalized signal, we can state that the PSD of its output  $S_{out,comp}(f)$  is equal to  $S_{out,eq}(f, A)$  for optimal equalization ( $A = A_{Opt}$ )

$$\begin{aligned}
S_{out,comp}(f) &= S_{in}(f) \cdot [H_{Ch}(jf)]^2 \cdot \left[ H_{Eq}(jf, A) \Big|_{A_{Opt}} \right]^2 \\
&= \left( \frac{\sin(\pi \cdot f)}{\pi \cdot f} \right)^2 \cdot \frac{P_{Eq}^2}{f^2 + P_{Eq}^2}
\end{aligned} \tag{2.17}$$

The adaptation loop uses two filters to select only a certain part of the spectrum. In this way, two different frequency ranges are compared. The accumulated power for comparison,  $P_{acc}(A)$ , can be obtained as the integral of  $S_{out,eq}(f, A)$  within the pass-band of the filters.

The sensitivity of the equalizer is given by how it reacts to changes in the boosting gain  $A$ ; therefore, the optimal frequency range for the filters in this design is that which maximizes it. To determine which frequency regions are the most susceptible to changes in  $A$ , the derivative of  $P_{acc}(A)$  with respect to  $A$  in the vicinity of  $A_{Opt}$  must be calculated

$$\begin{aligned}
\frac{\partial}{\partial A} P_{acc}(f) &= \frac{\partial}{\partial A} \left[ \int_0^\infty S_{out,eq}(f, A) \right]_{A=A_{Opt}} \\
&= \frac{\partial}{\partial A} \left[ \int_0^\infty S_{in}(f) \cdot [H_{Ch}(jf)]^2 \cdot [H_{Eq}(jf, A)]^2 \right]_{A=A_{Opt}}
\end{aligned} \tag{2.18}$$

Equation (2.18) has no analytic solution but it can be solved numerically. The choice of the filter characteristics for the implementation of a CT adaptive equalizer with a slicer must be made to maximize the product

$$P_{acc}^2(A) \cdot \frac{\partial}{\partial A} P_{acc}(A) \Big|_{A_{Opt}} \tag{2.19}$$

We shall particularize to two singular cases to see how the bandwidth of the filters should be chosen.

### Two HPFs

If two high pass filters (HPFs) are used, the limits of the integral range from the cut-off frequency of the filters to infinity; in practical terms the upper limit can be set to  $R_B$  as almost all spectral power is concentrated within the first lobe.

A plot of (2.18), (2.19), and the accumulated power for  $A_{Opt}$  is given in Fig. 2.11. It can be seen that the relative variation of the accumulated power for changes in  $A$  increases with the cut-off frequency. The increase is initially fast but its rate decreases to reach a limit value for cut-off frequencies close to the bit rate. This figure also shows how the accumulated power decreases as the cut-off frequency increases, which results from the fact that a narrower frequency range that, moreover, has less power is being taken into account. Examining the plot of (2.19) in Fig. 2.11, it can be seen how the frequency range that maximizes the sensitivity of the system spans around  $0.25 \cdot R_B$ .

On comparing it with values proposed in the literature, we see that in [HAR99] a cut-off frequency of 50 MHz is chosen for a 147 Mb/s signal, which agrees with the result obtained by the application of the criterion.

**Fig. 2.11** Frequency dependence of the variation of the accumulated power with respect to  $A$  (pointed), accumulated power for  $A_{Opt}$  (dashed), and their product (line) for CT adaptive equalizers with a slicer and two HPFs

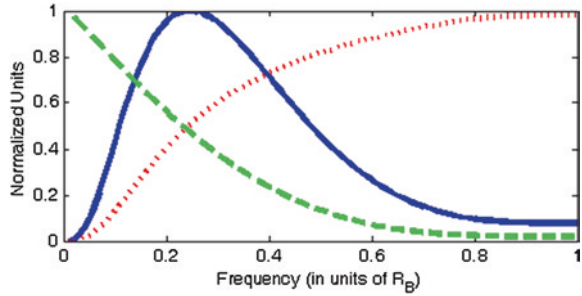
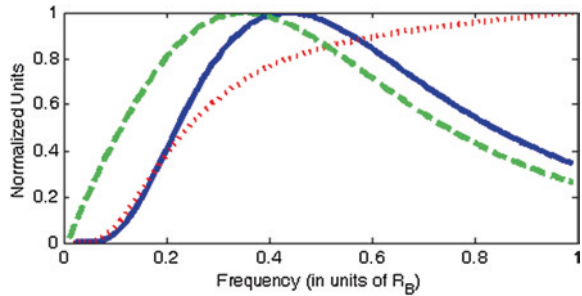


**Fig. 2.12** Frequency dependence of the variation of the accumulated power with respect to  $A$  (pointed), accumulated power for  $A_{Opt}$  (dashed), and its product (line) for CT adaptive equalizers with a slicer and two BPFs



## Two BPFs

In this case, the integral limits should be the upper and lower cut-off frequencies of the band pass filters (BPFs). The design of BPFs with a very narrow pass-band is challenging and results in power-hungry systems; since the equalizer has to adapt to process, voltage and temperature (PVT) variations, a pass-band of roughly 50 % of the BPF centre frequency is a typical choice [FAY08].

A plot of (2.18), (2.19), and the accumulated power for  $A_{Opt}$  is given in Fig. 2.12 for two BPFs. In a similar way to the previous case, the relative variation of the accumulated power increases as the centre frequency of the BPFs increases. This justifies the choice of a center frequency for the BPFs equal to the data bit rate made by [FAY08]. However, Fig. 2.12 shows that the power of the reference signal after filtering has a maximum at a frequency between 0.4 and 0.5 of the bit rate. Looking the plot of (2.19) in Fig. 2.12 it can be argued that, in reality, choosing a central frequency for the BPFs in the vicinity of  $0.5 \cdot R_B$  achieves a good trade-off between relative variations and total accumulated power for robustness and good sensitivity. This has been the choice made in [GON07], in which BPFs with a center frequency of 5 GHz have been chosen to equalize a 10 Gb/s bit stream.

## No Filters

Finally, in [CHE07, HOO04, YOO06, ZHA05], filters at the adaptation loop are eliminated altogether in an attempt to save power and area, and also to avoid the problems caused by filter mismatch and noise. Looking at Fig. 2.11, this situation

corresponds to minimum accumulated power relative variation, which suggests that the overall system sensitivity will be affected negatively; in fact, output rms jitter in [HOO04] is 11.4 % of the bit period, in [CHE07] is 5.3 %, in [ZHA05] is the 4 %, whereas it is only 2.2 % in [GON07], and 2.1 % in [FAY08].

### 2.3.2 CT Adaptive Equalizer with Spectrum-Balancing Technique

Like the previous case, the operation of CT adaptive equalizers with spectrum-balancing technique relies on the fact that the characteristics of the input to the communications system are known in advance. As the power ratio at different frequency ranges is constant, as shown in Chap. 1, we can control the adaptation loop using the information of the power spectrum at the output of the equalizer.

Several structures can be used to implement the comparison of the power at different frequency ranges. Some are shown in Fig. 2.13 which are realized by a LPF and a HPF [LEE06], a LPF and an APF [CHE10, HON10, SHI09, SUN05], two BPFs [MAX05], or two LPFs (that were first proposed for the authors of this work) [GIM13b]. Theoretically, any other combination of filters could be used. However, for different reasons they are not practicable. Consider as an example two HPFs. In this case, although they would select different parts of the spectrum and the comparison would be possible, both filters would take into account the high frequency region of the spectrum, and therefore, any change of the fiber characteristics would drastically affect both filter outputs; therefore, making the comparison rather unreliable.

When a LPF and a HPF are used to separate the frequencies for power comparison, their BWs are usually set at the frequency that separates the PSD of the ideal signal into two parts with equal power,  $f_m$ ; that is

$$\int_0^{f_m} T_B \left( \frac{\sin(\pi \cdot f \cdot T_B)}{\pi \cdot f \cdot T_B} \right)^2 df = \int_{f_m}^{\infty} T_B \left( \frac{\sin(\pi \cdot f \cdot T_B)}{\pi \cdot f \cdot T_B} \right)^2 df \quad (2.20)$$

In the case of an NRZ data stream this frequency can be found to be  $f_m = 0.28 \cdot R_B$  [LEE06]. If other modulation format is used, this value changes.

**Fig. 2.13** Some possible combination of filters for CT adaptive equalizer with spectrum-balancing technique

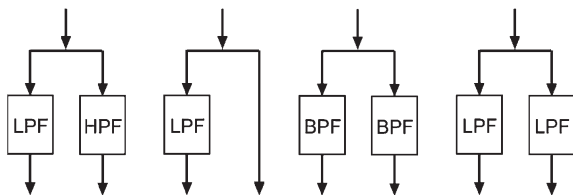
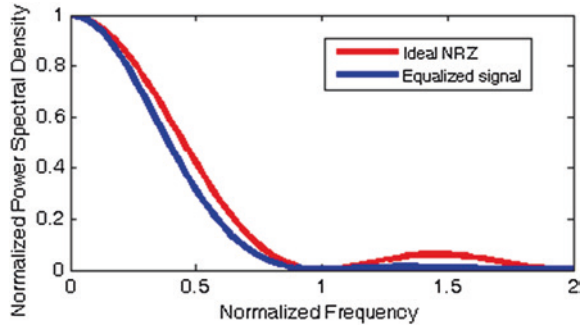


**Fig. 2.14** PSD of an ideal and an ideally equalized NRZ data stream



Although, in theory, any arbitrary frequency could be set to divide the spectrum of the data stream, the choice of the frequency that splits it into two parts with equal power avoids the need to re-scale the power of each part for proper comparison, which results in a simpler design.

When a different spectrum separation scheme is used, whether it is the combination of a low-pass and an all-pass filter, two band-pass filters, or two low-pass filters, the choice of the filter bandwidths is not straightforward, and typically a trial and error method is used by the designers. Moreover, in the case of BPFs, a trade-off has to be kept between spectrum requirements and power consumption. In fact, realizing the spectrum-balancing technique with BPFs greatly increases the total power consumption of the system, which has caused them to be relegated against other, preferred architectures [SHI09]. In the following, a general criterion will be extracted for a proper choice of these values.

### LPF-HPF

As mentioned, for this architecture, both filters are typically chosen to have a cut-off frequency equal to the frequency that separates the PSD into two parts with the same power. In the case of an NRZ stream, this frequency is  $0.28 \cdot R_B$ .

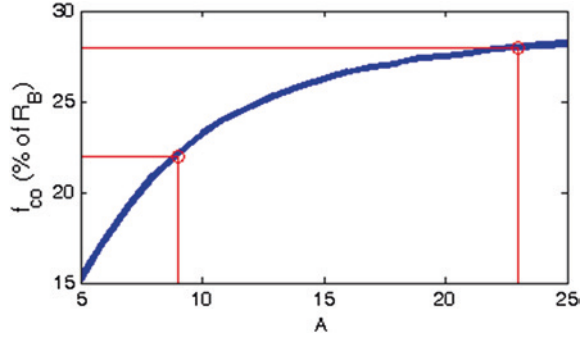
However, the use of the  $\text{sinc}^2$  function does not completely model the system because the actual PSD of the ideally equalized signal is affected by the equalizer pole (2.17). Figure 2.14 shows the comparison of the PSD of the resulting signal and that of the ideal NRZ stream. It can be seen how, despite being similar, high frequency components are over-attenuated. In this case, a frequency equal to  $0.28 \cdot R_B$  does not separate the PSD into two parts with equal power so this value must be recalculated.

Considering normalized frequencies, the expression that determines the proper cut-off frequency  $f_{co}$  with optimal gain  $A_{Opt}$  is given by

$$\int_0^{f_{co}} S_{out,eq}(f, A) \Big|_{A_{Opt}} df = \int_{f_{co}}^{\infty} S_{out,eq}(f, A) \Big|_{A_{Opt}} df \quad (2.21)$$

As an example, for the values used in this book, the cut-off frequency must be set at  $f_{co} = 0.22 \cdot R_B$ . Figure 2.15 shows how  $f_{co}$  changes according to  $A$ ; for a cut-off frequency of the filters equal to  $0.28 \cdot R_B$ , it is necessary that  $A_{Opt} = 23$ , which results in signal over-boost and thus non-optimal equalization and an increased SNR.

**Fig. 2.15** Dependency of  $f_{co}$  on  $A$  for spectrum-balancing technique with LPF and HPF.  $f_{co} = 0.28$  corresponds to  $A = 23$  whereas for  $A_{Opt} = 9$  a value of  $f_{co} = 0.22$  is obtained



### LPF-APF

In this case, as well as in all the remaining cases, the outputs of the two filters have different powers, so it is no longer possible to divide the PSD into two halves with equal power for direct comparison and power re-scaling is necessary by using some means of amplification.

To maximize sensitivity, we must use the range of frequencies with greater variation of accumulated power against variations of the boosting gain  $A$  in a manner similar to that used for the adaptive equalizer with a slicer.

The PSD of the signal after the line equalizer was given in (2.16). If its derivative with respect to the boosting gain  $A$  is calculated around the optimal gain  $A_{Opt}$ , the resulting expression will indicate which frequency changes in  $A$  produce larger changes in the total PSD. So, if the derivative with respect to the frequency  $f$  of that expression particularized for the optimal adaptation gain  $A_{Opt}$  is obtained and equalling to 0, that yields (2.22); from it, the value of the frequency  $f_{max}$  for maximum sensitivity against changes in  $A$  around  $A_{Opt}$  can be obtained.

$$\frac{\partial}{\partial f} \left[ \frac{\partial}{\partial A} S_{out,eq}(f, A) \Big|_{A_{Opt}} \right] = 0 \rightarrow f_{max} \quad (2.22)$$

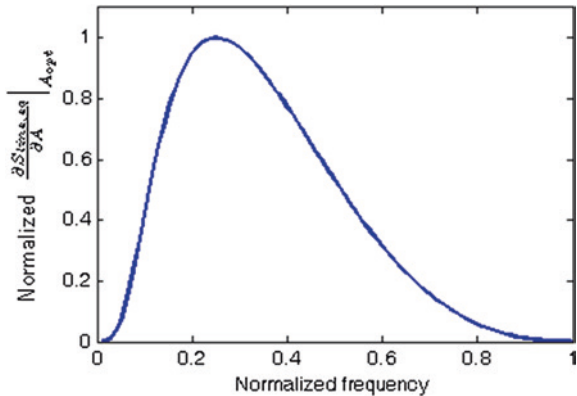
Frequencies around  $f_{max}$  must be used to select the pass-bands of the filters to maximize the sensitivity to variations in the spectrum of the signal. That is, one of the filters has to give way to frequencies around  $f_{max}$  while the other has to block them.

To illustrate this behavior, let us substitute the numerical values in (2.22). It can be seen in Fig. 2.16 that the maximum variation is achieved for a frequency slightly above 20 % of the bit data rate, a value that will be taken as a reference to establish the filter bandwidth criterion.

As the APF lets all frequencies through, the LPF has to block those in the range of  $f_{max}$ . This way, the criterion is that its cut-off frequency should be placed well below it. This way, only the all-pass filtered signal will have the maximum accumulated power variation.

If this result is compared to adaptive equalizer designs reported in the literature, it can be seen that the LPF bandwidth typically lies well below the data rate. For example, in [HON10] a bandwidth of 100–150 MHz for a 1 Gb/s signal is

**Fig. 2.16** Variation of the PSD of the equalized signal with respect to  $A$  at  $A_{Opt}$ . The maximum variation is obtained for  $f$  just above  $0.2 \cdot R_B$



proposed to the LPF, in [SUN05] a bandwidth of 15 MHz for a 20 Gb/s signal, in [CHE10] a bandwidth of 527 MHz for a 5 Gb/s signal, in [GIM13a] a bandwidth of 130 MHz for a 2.5 Gb/s signal, whereas [SHI09] sets the bandwidth at 100 MHz for a 5 Gb/s signal. These results agree with the proposed criterion.

### Two BPFs

Similarly, in the case of two BPFs, the choice of their BWs must be carried out so that the frequencies that correspond to maximum  $\frac{\partial}{\partial A} S_{out,eq}(f, A)|_{A_{Opt}}$  are blocked by one of the filters and let through by the other for enhanced comparison. According to this, one of the BPFs must have its pass-band centered on  $f_{max}$  whereas for the other BPF it should be placed either well above  $f_{max}$  or well below it. To facilitate the design of the BPF while saving area and power, it is preferable to choose a pass-band well below  $f_{max}$ .

If this result is compared with adaptive equalizer designs reported in the literature, in [MAX05] values of 200 and 600 MHz for a 3.2 Gb/s signal have been chosen, which corresponds to  $0.06 \cdot R_B$  and  $0.19 \cdot R_B$ , which is in agreement with the proposed criterion where  $f_{max} = 0.2 \cdot R_B$ .

### Two LPFs

Following the argument used so far, the bandwidth of the two LPFs must be chosen so that one of them blocks the frequencies that maximize  $\frac{\partial}{\partial A} S_{out,eq}(f, A)|_{A_{Opt}}$  while the other lets them through. That is, one LPF should have a bandwidth well below  $f_{max}$  whereas for the other one, a value roughly above  $f_{max}$  will suffice since the contribution to accumulated power of higher frequencies is small and does not compensate for the design challenge and higher power consumption of a LPF with a higher cut-off frequency.

If this result is compared with adaptive equalizer designs reported in the literature, in [GIM13b], the cut-off frequencies of the LPFs are set to 15 and 300 MHz for a system operating at 1.25 Gb/s. These values correspond to  $0.01 \cdot R_B$  and  $0.24 \cdot R_B$ , which agrees with the proposed criteria.

**Table 2.1** Comparison between theoretical results and published papers

Adaptation loop structure	Theoretical results	Published results	References
<b>Slicer and two HPFs</b>	$f_{HPF} \approx 0.25 \cdot R_B$	$f_{HPF} = 0.34 \cdot R_B$	[HAR99]
<b>Slicer and two BPFs</b>	$f_{BPF} \approx (0.4 - 0.5) \cdot R_B$	$f_{BPF} = 0.5 \cdot R_B$	[GON07]
<b>Spectrum-balancing technique with LPF-APF</b>	$f_{LPF} \ll 0.2 \cdot R_B$	$f_{LPF} = 0.1 \cdot R_B$	[HON10]
		$f_{LPF} = 7.5 \cdot 10^{-4} \cdot R_B$	[SUN05]
		$f_{LPF} = 0.1 \cdot R_B$	[CHE10]
		$f_{LPF} = 0.05 \cdot R_B$	[GIM13a]
		$f_{LPF} = 0.02 \cdot R_B$	[SHI09]
<b>Spectrum-balancing technique with 2 BPFs</b>	$f_{BPF1} \ll 0.2 \cdot R_B$	$f_{BPF1} = 0.06 \cdot R_B$	[MAX05]
	$f_{BPF2} \approx 0.2 \cdot R_B$	$f_{BPF2} \approx 0.19 \cdot R_B$	
<b>Spectrum-balancing technique with 2 LPFs</b>	$f_{LPF1} \ll 0.2 \cdot R_B$	$f_{LPF1} = 0.01 \cdot R_B$	[GIM13b]
	$f_{LPF2} > 0.2 \cdot R_B$	$f_{LPF2} \approx 0.24 \cdot R_B$	

### 2.3.3 Summary

Table 2.1 summarizes the theoretical criterion for the filters bandwidth selection in every case and compares them with the values used in literature. The values obtained according to the criteria coincide with the ad hoc values proposed in the literature.

## 2.4 Loop Filter Selection Criteria

We have explained how to select the BW of the loop filters; but, how can we choose between different filter combinations?

To compare different possibilities, the four adaptation loop configurations previously shown were built using Simulink<sup>®</sup>. To make the simulations more realizable, a second pole has been included in the split-path configuration of the equalizer. A tunable zero has also been included. The structure using a slicer has been disregarded as it increases circuit complexity, power dissipation and area consumption since it requires generating sharper rising and falling edges of the signal entering from the line equalizer [CHE10, LEE09].

We use a 1 Gb/s NRZ PRBS with  $2^{31} - 1$  maximum length. This sequence passes through a block that simulates the behavior of a Mitsubishi GH SI-POF, whose frequency response for different fiber lengths was shown in Fig. 1.21. The signal at the input of the equalizer is shown in Fig. 2.17, where ISI can clearly be observed. At 0.1  $\mu$ s a change in the fiber length is produced. Note that the ISI is more acute after the length increase.

To verify the proper operation of the adaptive loop we change the length  $L$  of the fiber at a certain time and observe how both the output of the equalizer and the control signal used to modify the response of the equalizer change. Figure 2.18

**Fig. 2.17** Equalizer input signal for two different POF lengths:  $L = 10$  m from 0 to  $0.1 \mu\text{s}$  and  $L = 40$  m from  $0.1$  to  $0.2 \mu\text{s}$

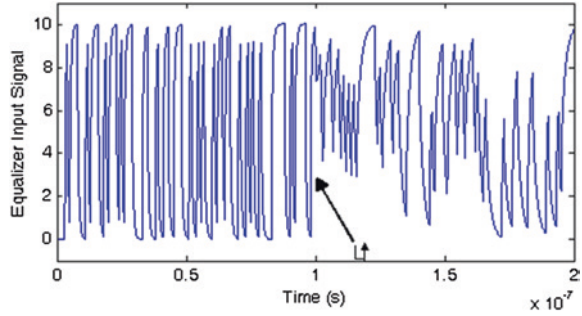
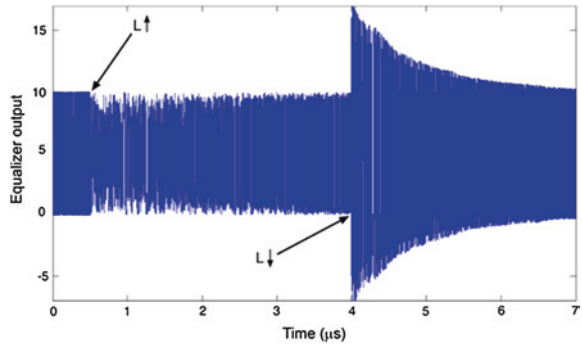


**Fig. 2.18** Adaptive equalizer output for length changes:  $L \uparrow = +30$  m and  $L \downarrow = -30$  m



shows the output of the equalizer and how it evolves when the fiber length increases  $+30$  m or decreases  $-30$  m. Figure 2.19 shows the control signal that is carried to the equalizer to change its response.

To compare the different filter combinations used in the implementation of the spectrum-balancing loop we measure the rise and fall times ( $T_R$  and  $T_F$ ), defined as the times that the control signal takes to go from 10 to 90 % of the total change. Table 2.2 compares these times in each of the stages when the variance<sup>2</sup> in all the configurations is the same. It also shows the constant time of the integrator  $T_{INT}$  used in the adaptation loop to generate a clean dc signal to modify the response of the equalizer, because this is a critical parameter in the implementation of the loop as it is related with the area consumption.

The integrator conditions were forced so that the adaptive equalizers could respond to abrupt changes in the conditions of the fiber. In the practice, we will not have such an abrupt change. Therefore, bigger capacitors could be used to obtain a cleaner control signal. These bigger capacitors can be implemented off-chip.

It can be seen that the worst configuration is to use two BPFs, because it has the worst rise and fall times. Moreover, realizing the spectrum-balancing technique with BPFs severely increases the total power consumption of the system.

<sup>2</sup> Variance: Difference between the maximum and minimum value in the stationary state.

**Fig. 2.19** Example of control signal for length changes:  $L \uparrow = +30$  m and  $L \downarrow = -30$  m

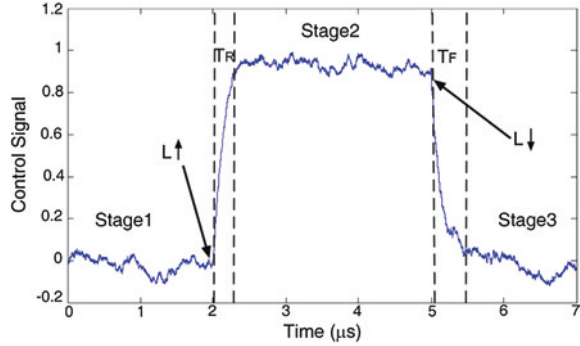


**Table 2.2** Comparative analysis between the different filters configurations. The rise time  $T_R$ , fall time  $T_F$  and constant time of the used integrator  $T_{INT}$  are compared

Filter	$T_R$ ( $\mu s$ )	$T_F$ ( $\mu s$ )	$T_{INT}$ ( $\mu s$ )
LPF-APF	2.43	3.76	500
LPF-HPF	3.26	6.36	1,000
BPF-BPF	6.70	6.42	48
LPF-LPF	3.06	5.02	500

Therefore, it has been relegated against other preferred architectures. The LPF-HPF configuration also has higher rise and fall times than the other two alternatives (LPF-APF and LPF-LPF). It would also require a double size capacitor in the integrator as the  $T_{INT}$  is double. Implementing a HPF usually requires higher power consumption than a LPF. The LPF-APF and LPF-LPF combinations are good choices as they have similar rise and fall times. So, choosing between them depends on the structures used to implement them as well as other parameters such as the variation of the filters with PVT, the matching between the filters, etc.

## 2.5 Conclusions

In this chapter, the theoretical fundamentals of a class of adaptive continuous-time equalizers have been explained.

First of all, we have provided a basic analysis of the transfer function of the equalizers and explained how the limited frequency response of the channel is compensated.

Then the spectrum of the incoming data has been studied. NRZ is the simplest and the most widely used code, and is therefore the data stream to be going to be used in the following chapters. The normalized power spectral density and how it is affected by different filtering has been shown.

A detailed analysis of the effect of continuous-time adaptive equalizers on the PSD of the incoming signal has been made to formulate general design criteria for

the bandwidth of the filters used to implement the adaptation loop. First, a unified treatment in the frequency domain has been presented which is valid for the two main continuous-time adaptive equalization techniques: with both a slicer and the spectrum-balancing technique. In all cases, with the help of either the PSD of the equalized signal or the accumulated power versus frequency, conditions for maximum sensitivity have been used to derive mathematical expressions to obtain the optimal filter bandwidth.

The results have been obtained using frequencies normalized to the data bit rate, which allows a more general formulation of the design criteria. Moreover, these results have been compared with the values reported in recently published works in the field. The conclusion is that the values obtained according to the criteria coincide with the ad hoc values proposed in the literature. This way, we have provided a methodology that can be applied to any other set of conditions, thus facilitating designers the task of choosing the proper loop filters bandwidth in continuous-time adaptive equalizers.

It is important to mention here that the spectrum-balancing technique is valid as long as the PSD of the incoming data stream is known. Therefore, the performed study can be applied to other modulation formats, such as duo-binary and 4-PAM and to other codifications such as return to zero (RZ).

Finally, a functional simulation of the adaptation loop has been provided to obtain a way to choose between different filter combinations. The structure using a slicer was disregarded because it increases circuit complexity, power dissipation and area consumption. So, the filter combinations in an architecture that uses the spectrum-balancing technique were studied. We found that the LPF-APF and the LPF-LPF are the best configurations. Choosing between them will depend on the structures used to implement them as well as other parameters such as PVT variation of the filters, matching between the filters, etc.

Thus, the contents of this chapter let us deal with the design of a continuous-time adaptive equalizer, which is the focus of this book.

## References

- [BEY08] W. Beyene, The design of continuous-time linear equalizers using model order reduction techniques, in Proceedings of IEEE Electrical Performance of Electronic Packaging (IEEE-EPEP), pp. 187–190, Oct 2008
- [CHE07] W.-Z. Chen, S.-H. Huang, G.-W. Wu, C.-C. Liu, Y.-T. Huang, C.-F. Chiu, W.-H. Chang, Y.-Z. Juang, A 3.125 Gbps CMOS fully integrated optical receiver with adaptive analog equalizer, in IEEE Asian Solid-State Circuits Conference 2007 (ASSCC'07), pp. 396–399, Nov 2007
- [CHE10] K.-H. Cheng, Y.-C. Tsai, Y.-H. Wu, Y.-F. Lin, A 5-Gb/s Inductorless CMOS adaptive equalizer for pci express generation II applications. IEEE Trans. Circuits Syst. II Express Briefs **57**(5), 324–328 (2010)
- [FAY08] A.A. Fayed, M. Ismail, A low-voltage low-power CMOS analog adaptive equalizer for UTP-5 cables. IEEE Trans. Circuits Syst. I Regul. Pap. **55**(2), 480–495 (2008)
- [GIM13a] C. Gimeno, E. Guerrero, C. Aldea, S. Celma, A 2.5 Gb/s low-voltage CMOS fully-differential adaptive equalizer, in Proceedings of 2013 SPIE Microtechnologies Conference (SPIE 2013), pp. 876402-1–876402-8, Apr 2013

- [GIM13b] C. Gimeno, C. Sánchez-Azqueta, E. Guerrero, C. Aldea, S. Celma, A 1-V 1.25-Gbps CMOS analog front-end for short reach optical links, in IEEE European Solid-State Circuits Conference (ESSCIRC2013), pp. 339–342, Sept 2013
- [GON07] S. Gondi, B. Razavi, Equalization and clock and data recovery techniques for 10-Gb/s CMOS serial-link receivers. IEEE J. Solid-State Circuits **42**(9), 1999–2011 (2007)
- [GOO85] J.W. Goodman, *Statistical optics* (Wiley, New York, 1985)
- [HAR99] G. Hartman, K. Martin, A. McLaren, Continuous-time adaptive analog coaxial cable equalizer in 0.5  $\mu\text{m}$  CMOS, in Proceedings of the 1999 IEEE International Symposium on Circuits and Systems (ISCAS99), pp. 97–100, Jul 1999
- [HAY01] S. Haykin, *Communication Systems*, 4th edn (Wiley, New York, 2001)
- [HOL06] T. Hollis, D. Comer, Mitigating ISI through selfcalibrating continuous-time equalization. IEEE Trans. Circuits Syst. I Regul. Pap. **53**(10), 2234–2245 (2006)
- [HON10] D. Hong, S. Saberi, K.-T. Cheng, C. P. Yue, A two-tone test method for continuous-time adaptive equalizers, in *Efficient Test Methodologies for High-Speed Serial Links* (Springer, Berlin, 2010), pp. 75–87
- [HOO04] L. Hoon, H. Gunhee, A low power and small area analog adaptive line equalizer for 100 Mb/s data rate on UTP cable. IEICE Trans. Electron. **87**(4), 634–639 (2004)
- [LEE06] J. Lee, A 20-Gb/s adaptive equalizer in 0.13- $\mu\text{m}$  CMOS technology. IEEE J. Solid-State Circuits **41**(9), 2058–2066 (2006)
- [LEE09] D. Lee, J. Han, G. Han, S.M. Park, 10 Gbit/s 0.0065  $\text{mm}^2$  6 mW analogue adaptive equalizer utilising negative capacitance, in IEEE International Solid-State Circuits Conference (ISSCC), pp. 190–191, Feb 2009
- [MAX05] Maxim Integrated Products, *3.2 Gbps Equalizer and Cable Driver* (2005)
- [SAN11] C. Sánchez-Azqueta, S. Celma, A phase detection scheme for clock and data recovery applications, in Proceedings of the 20th IEEE European Conference on Circuit Theory and Design (ECCTD2011), pp. 130–133, Aug 2011
- [SAN13] C. Sánchez-Azqueta, C. Gimeno, S. Celma, A comparative study of continuous-time analog adaptive equalizers, in Proceedings of the 2013 SPIE Microtechnologies Conference (SPIE 2013), vol. 8764, pp. 876402-8, Apr 2013
- [SAN14] C. Sánchez-Azqueta, C. Gimeno, E. Guerrero, C. Aldea, S. Celma, Design considerations for loop filters in continuous-time adaptive equalizers, in Proceedings of the International Multi-Conference on Systems, Signals and Devices (SSD 2014), Feb 2014
- [SHI09] D.H. Shin, J.E. Jang, F. O'Mahony, C.P. Yue, A 1-mW 12-Gb/s continuous-time adaptive passive equalizer in 90-nm CMOS, in Proceedings of the IEEE Custom Integrated Circuits Conference (CICC09), pp. 117–120, Sept 2009
- [SUN05] R. Sun, A low-power 20-Gb/s continuous-time adaptive passive equalizer. Thesis, B.S. Tsinghua University 1999, Dec 2005
- [YOO06] K. Yoo, G. Han, H. Yoon, Convergence analysis of the cascade second-order adaptive line equalizer. IEEE Trans. Circuits Syst. II Express Briefs **53**(6), 507–511 (2006)
- [ZHA05] G.E. Zhang, M.M. Green, A 10 Gb/s BiCMOS adaptive cable equalizer. IEEE J. Solid-State Circuits **40**(11), 2132–2140 (2005)

CMOS Continuous-Time Adaptive Equalizers for  
High-Speed Serial Links

Gimeno, C.; Celma, S.; Aldea, C.

2015, XXII, 148 p. 136 illus., 85 illus. in color., Hardcover

ISBN: 978-3-319-10562-8